

A Novel Treatment of the Josephson Effect

Jacob Szeftel^{1,*}, Nicolas Sandeau², and Michel Abou Ghantous³

¹ENS Paris-Saclay/LuMIn, 4 avenue des Sciences, 91190 Gif-sur-Yvette, France

²Aix Marseille Univ, CNRS, Centrale Marseille, Institut Fresnel, F-13013 Marseille, France and

³American University of Technology, AUT Halat, Highway, Lebanon

A new picture of the Josephson effect is devised. The radio-frequency (RF) signal, observed in a Josephson junction, is shown to stem from bound electrons, tunneling periodically through the insulating film. This holds also for the microwave mediated tunneling. The Josephson effect is found to be conditioned by the same prerequisite worked out previously for persistent currents, thermal equilibrium and occurrence of superconductivity. The observed negative resistance behaviour is shown to originate from the interplay between normal and superconducting currents.

PACS numbers: 74.50.+r, 74.25.Fy, 74.25.Sv

I. INTRODUCTION

The Josephson effect was initially observed^{1,2} in the kind of circuit sketched in Fig.1 and has kept arousing an unabated interest, in particular because of its relevance to electronic devices^{3,4} and quantum computation⁵⁻⁷. For simplicity, both superconducting leads A, B are assumed here to be made out of the same material. They are separated by a thin ($< 10\text{\AA}$) insulating film, enabling electrons to tunnel through it. If A, B were made of a normal metal, a constant current $I = \frac{U_s}{R+R_t}$ would flow through the circuit. Nevertheless, this simple setup has attracted considerable attention because of Josephson's predictions⁸ :

1. there should be $\langle I \rangle \neq 0$ for $\langle U \rangle = 0$, which entails $\left| \frac{d\langle I \rangle}{d\langle U \rangle} (\langle U \rangle = 0) \right| \rightarrow \infty$ ($\langle I \rangle, \langle U \rangle$ refer to time t averaged values of $I(t), U(t)$);
2. $I(t), U(t)$ should oscillate at frequency $\omega = \frac{2e\langle U \rangle}{\hbar}$ with e being the electron charge.

However, claim 1 seems to disagree with experimental data, reproduced in Fig.2, because $\frac{d\langle I \rangle}{d\langle U \rangle} (\langle U \rangle = 0) \approx .06\Omega^{-1}$ is seen to be *finite*.

In addition, claim 1 appears *questionable* in view of the demurrals below :

- $\langle U \rangle = 0$ implies that there is *no electric field*, available to accelerate the conduction electrons. Hence the *finite* momentum, associated with the tunneling current $\langle I \rangle \neq 0$, has built up with *no external force*, which *violates* Newton's law;
- since the electrons undergo *no electric field*, it is hard to figure out why the tunneling current should flow into *one* direction rather than the *opposite* one;
- $\langle I \rangle \neq 0$ despite $U_s = \langle U \rangle = 0$ entails that the t averaged circulation of the electric field along the closed circuit, pictured in Fig.1, equals $R\langle I \rangle \neq 0$ and thence the electric field is bound to be induced by a t dependent magnetic field, according to the

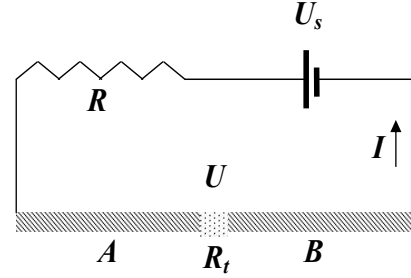


FIG. 1. Sketch of the electrical setup, operated to study the Josephson effect. The Josephson capacitor consists in two superconducting electrodes A, B (hatched area) straddling an insulating film (dotted area); the insulator thickness has been hugely magnified for the reader's convenience. U_s, U, R, R_t stand, respectively, for the constant applied bias, the voltage drop across the capacitor, a loading resistor inserted to measure the total current I and the tunneling resistance, defined in section II.

Faraday-Maxwell equation, in contradiction with the experimental setup in Fig.1, involving *no t dependent magnetic field*.

Besides a periodic signal was indeed observed^{1,9}, but in the *RF range*, i.e. $\omega < 100\text{MHz}$, rather than in the *microwave* one, i.e. $\omega > 1\text{GHz}$, as inferred from Josephson's formula, given the measured $\langle U \rangle$ values.

Consequently, the numerous experimental data, documenting the electrodynamical behaviour of the Josephson junction^{3,4}, have been interpreted so far by resorting⁹ to a formula, relating $I(t), U(t)$ to Ginzburg and Landau's phase¹⁰ Φ_{GL} . However the time behaviour of $\Phi_{GL}(t)$ has been derived with help of a perturbation calculation^{8,11-14}, which is well-suited to describe the *random* tunneling of a single particle, either electron or Bogolyubov-Valatin excitation^{13,14}, but cannot account for the *coherent* tunneling of *bound* electrons, such as those making up the superconducting state¹⁵⁻¹⁹, for some reason to be given below. Therefore, this work is rather intended at presenting an *alternative* explanation of the Josephson effect, *unrelated* to Φ_{GL} , by studying the *time-*

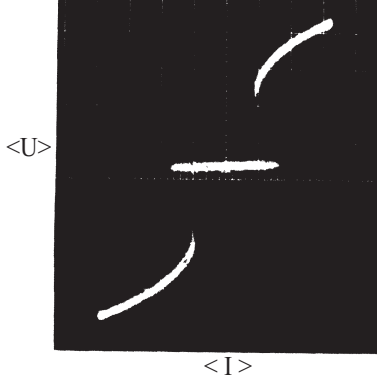


FIG. 2. Characteristic $I(U)$ recorded by Shapiro¹ and used here with APS permission; vertical scale is $58.8\mu V/cm$, horizontal scale is $130nA/cm$.

periodic tunneling motion²⁰ of bound electron pairs^{15–19} through the insulating barrier.

The outline is as follows : the expression of the tunneling current, conveyed by independent electrons, is recalled in section II, whereas the current carried by bound electrons is worked out in section III; this enables us to solve, in section IV, the electrodynamical equation of motion of the circuit, depicted in Fig.1; sections V, VI deal respectively with the microwave mediated Josephson effect^{1,2} and the negative resistance induced signal⁹. The results are summarised in the conclusion.

II. RANDOM TUNNELING

As in our previous work^{15–19,21–23}, the present analysis will proceed within the framework of the two-fluid model, for which the conduction electrons comprise superconducting and independent electrons, in respective concentration c_s, c_n . The superconducting and independent electrons are organized, respectively, as a many bound electron¹⁶ (MBE), BCS-like²⁴ state, characterised by its chemical potential μ , and a degenerate Fermi gas²⁵ of Fermi energy E_F . Assuming $U = U_A - U_B$, $eU > 0$, the current, conveyed by the independent electrons, will flow from A toward B and there is $eU = E_F^A - E_F^B$, with E_F^A, E_F^B being the Fermi energy in electrodes A, B , respectively. Hence, since the experiments are carried out at low temperature, the corresponding current density j_n is inferred from the properties of the Fermi gas²⁵ to read

$$j_n = \frac{e^2 \rho(E_F^A) v_F T}{2} U \Rightarrow R_t \propto \frac{1}{\rho(E_F^A)} \quad , \quad (1)$$

with $\rho(E_F)$, v_F , T standing for the one-electron density of states at the Fermi level, the Fermi velocity and the one-electron transmission coefficient through the insulating barrier ($\Rightarrow 0 < T < 1$). Several remarks are in order, regarding Eq.(1)

- Eq.(1) is seen to agree with the corresponding formula, available in textbooks^{13,14},
- the independent electrons contribute thence the current $I_n(t) = U(t)/R_t$ to the total current $I(t)$. However, despite I_n obeying Ohm's law, the tunneling electrons suffer no energy loss inside the insulating barrier;
- because c_n is expected to grow¹⁶ at the expense of c_s with growing $|I|$, this implies that $\rho(E_F)$ and R_t will, respectively, increase and decrease with increasing $|I|$. The negative resistance effect, addressed in section 6, stems from this property.

III. COHERENT TUNNELING

Unlike the random diffusion of independent electrons across the insulating barrier, the tunneling motion of bound electrons takes place as a time-periodic oscillation to be analysed below. Their energy per unit volume \mathcal{E} depends¹⁵ on c_s only and is related to their chemical potential μ by $\mu = \frac{\partial \mathcal{E}}{\partial c_s}$. Before any electron crosses the barrier, the total energy of the whole bound electron system, including the leads A, B , reads

$$\mathcal{E}_i = 2\mathcal{E}(c_e) + ec_e U \quad , \quad (2)$$

with c_e referring to the bound electron concentration at thermal equilibrium. Let $n \gg 1$ of bound electrons cross the barrier from A toward B . The total energy becomes

$$\mathcal{E}_f = \mathcal{E}(c_e + \frac{n}{V}) + \mathcal{E}(c_e - \frac{n}{V}) + e(c_e - \frac{n}{V})U \quad , \quad (3)$$

with V being the volume, taken to be equal for both leads A, B . Energy conservation requires $\mathcal{E}_i = \mathcal{E}_f$, which leads finally to

$$n = \frac{eV}{\frac{\partial \mu}{\partial c_s}(c_e)} U \quad . \quad (4)$$

The wave-functions φ_i, φ_f , associated with the twofold degenerate eigenvalue $\mathcal{E}_i = \mathcal{E}_f$, read

$$\begin{aligned} \varphi_i &= \varphi_A(c_e) \otimes \varphi_B(c_e) \\ \varphi_f &= \varphi_A(c_e - \frac{n}{V}) \otimes \varphi_B(c_e + \frac{n}{V}) \end{aligned} \quad , \quad (5)$$

with $\varphi(c_s)$ being the MBE, c_s dependent eigenfunction^{16,19,24}. The coherent tunneling motion of n electrons across the barrier is thence described by the wave-function $\psi(t)$, solution of the Schrödinger equation

$$\begin{aligned} i \frac{\partial \psi}{\partial t} &= H \psi \\ H &= \omega_t \sigma_x \quad , \quad \omega_t = \langle \varphi_i | V_b | \varphi_f \rangle \end{aligned} \quad . \quad (6)$$

The Hamiltonian H and the potential barrier V_b , hindering the electron motion through the Josephson junction

and including the applied voltage U , are expressed in frequency unit, $\frac{V\mathcal{E}_i}{\hbar}$ is taken as the origin of energy, whereas ψ and the Pauli matrix²⁶ σ_x have been projected onto the basis $\{\varphi_i, \varphi_f\}$. The tunneling frequency ω_t , taken to lie in the RF range, i.e. $\omega_t < 100\text{MHz}$, as reported by Shapiro¹, is realized to describe the tunneling motion of *bound* electrons in a similar way as the matrix element T_{kq} does for the *random* tunneling of a *single* electron in the mainstream view^{13,14}. Finally Eq.(6) is solved²⁶ to yield

$$\psi(t) = \cos\left(\frac{\omega_t t}{2}\right) \varphi_i - i \sin\left(\frac{\omega_t t}{2}\right) \varphi_f \quad , \quad (7)$$

whence the charge $Q_s, -Q_s$, piling up in A, B respectively, is inferred, thanks to Eq.4, to read

$$Q_s(t) = -ne |\langle \psi(t) | \varphi_f \rangle|^2 = C_e U \sin^2\left(\frac{\omega_t t}{2}\right) \quad ,$$

with the effective capacitance C_e defined as

$$C_e = -\frac{e^2 V}{\frac{\partial \mu}{\partial c_s}(c_e)} \quad .$$

Since $\frac{\partial \mu}{\partial c_s} < 0$ has been shown to be a prerequisite for the existence of persistent currents¹⁵, thermal equilibrium¹⁶ and occurrence of superconductivity^{18,19}, it implies that $C_e > 0$. In addition, given the estimate¹⁶ of $\frac{\partial \mu}{\partial c_s}$, it may take a very large value up to $C_e \approx 1F$. At last, by contrast with I_n being incoherent, the bound electrons contribute an *oscillating* current $I_s(t) = \dot{Q}_s = \frac{dQ_s}{dt}$ to $I(t)$.

The marked difference between the *random* diffusion current $I_n(t)$ and the *time-periodic* one $I_s(t)$ ensues from the property that energy must be *conserved* during tunneling. This is automatically ensured^{13,14} for an independent particle because its eigenenergy is defined uniquely all over the electrodes A, B and the insulating barrier, whereas special care, as expressed in Eq.(4), must be taken to enforce energy conservation for *bound* electrons tunneling through a barrier. Unfortunately this *crucial* constraint has been *overlooked* in the mainstream analysis^{8,11-14}.

IV. ELECTRODYNAMICAL BEHAVIOUR

The total current $I(t)$ comprises 3 contributions, namely $I_n = \frac{U}{R_t}, I_s = \dot{Q}_s$ and a component $C\dot{U}$, loading the Josephson capacitor (C refers to its capacitance), so that the electrodynamical equation of motion reads

$$U_s = U + RI \quad , \quad I = \frac{U}{R_t} + \dot{Q}_s + C\dot{U} \quad ,$$

which is finally recast into

$$\dot{U} = \frac{U_s - U \left(1 + \frac{R}{R_t} + \frac{RC_e \omega_t}{2} \sin(\omega_t t)\right)}{R \left(C + C_e \sin^2\left(\frac{\omega_t t}{2}\right)\right)} \quad . \quad (8)$$

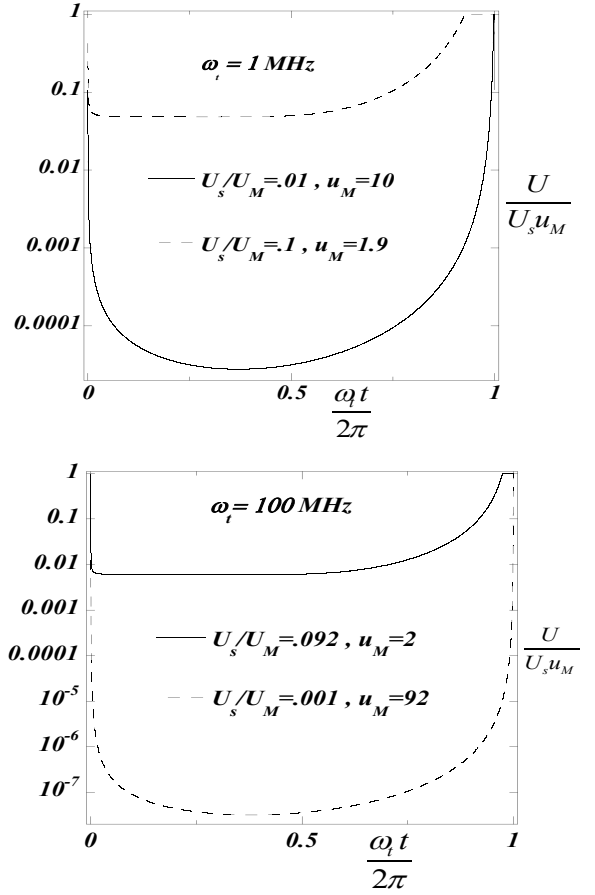


FIG. 3. Semi-logarithmic plots of the periodic solution $U(t)$ of Eq.(8), calculated for $\omega_t = 1\text{MHz}, 100\text{MHz}$ and $I_M = 1\text{mA}, 0.1\text{mA}$; $U_M = (R + R_n) I_M$ and u_M is the maximum value of $\left| \frac{U(t \in [0, \frac{2\pi}{\omega_t}])}{U_s} \right|$.

It is worth noticing that, due to $\left| \frac{C_e}{C} \right| \gg 1$, the denominator in the right-hand side of Eq.(8) would vanish for $C_e < 0$, at some t value, so that Eq.(8) cannot be solved unless $C_e > 0 \Rightarrow \frac{\partial \mu}{\partial c_s} < 0$, which confirms a *previous*¹⁵⁻¹⁹ conclusion, derived independently.

$\left| \frac{\partial \mu}{\partial c_s} \right|$ is expected¹⁶ to increase with increasing $|I|$ and is no longer defined for $|I| > I_M$, the maximum value of the bound electron current, because the sample goes thereby normal. Consequently for practical purposes, Eq.(8) has been solved by assuming $R_t (|I| \leq I_M) = R_0 g\left(\left|\frac{I}{I_M}\right|\right) + R_n$, $R_t (|I| > I_M) = R_n$ with $\frac{R_0}{R_n} \gg 1$, $C_e (|I| \leq I_M) = C_0 g\left(\left|\frac{I}{I_M}\right|\right)$, $C_e (|I| > I_M) = 0$ with $\frac{C_0}{C} \gg 1$, and $g(x) = 1 - x^2$. Regardless of the initial condition $U(0)$, the solution $U(t)$ of Eq.(8) becomes time-periodic, i.e. $U(t) = U\left(t + \frac{2\pi}{\omega_t}\right), \forall t$, after a short transient regime.

Eq.(8) has been solved with the assignments $C = 1\text{pF}, C_0 = 1\text{mF}, R = 10\Omega, R_n = 100\Omega, R_0 = 10\text{K}\Omega$, and

the corresponding $U(t)$ have been plotted in Fig.3. The large slope $|\frac{dU}{dt}(0)| \gg 1$ stems from $\frac{C_0}{C} \gg 1$. Since no experimental data of $U(t)$ have been reported in the literature to the best of our knowledge, no comparison between observed and calculated results can be done. Nevertheless, the large $u_M \gg 1$ values, seen in Fig.3, have been indeed observed¹. Likewise, the calculated u_M values have been found to increase very steeply with U_s decreasing toward 0. Hence the thermal noise, generated by the U_s source, will suffice even at $U_s = 0$ to give rise to sizeable u_M , which is likely to be responsible for the *misconception*⁸, conveyed by hereabove mentioned claim 1. As a matter of fact, the noisy behaviour of the circuit sketched in Fig.1 has been reported¹.

The characteristics $I(U)$, plotted in Fig.4, have been reckoned as

$$\langle f \rangle = \frac{\omega}{2\pi} \int_0^{2\pi} f(u) du \quad ,$$

with $f = U, I$. In all cases, there is $\langle I \rangle(0) = 0$ with *finite* $\frac{d\langle I \rangle}{d\langle U \rangle}(0)$ in agreement with the experimental data in Fig.2. However the slope $\frac{d\langle I \rangle}{d\langle U \rangle}(0)$, calculated for $\omega_t = 100\text{MHz}$, is much larger than the one at $\omega_t = 1\text{MHz}$.

Noteworthy is that there are no observed $\langle I \rangle$ data in Fig.2 over a broad $\langle U \rangle$ range, starting from $\langle U \rangle \approx 0$ up to a value big enough for the sample to go into the normal state, characterised by constant $I = I_n > I_M$. This feature might result¹ from $U_s \propto \sin(\omega_p t)$ with $\omega_p = 60\text{Hz}$. Thus since the tunneling frequency ω_t is expected to decrease exponentially^{13,14,20} with increasing n and thence U , this entails that the signal could indeed no longer be observed for $\omega_t < \omega_p$. Likewise, the observed frequency modulation^{2,13,14}, i.e. $\omega_t(n)$ is time-periodic, ensues from $n(t) \propto U(t)$ being time-periodic too (see Eq.(4)). At last, it is in order to realize that the characteristics $I(U)$ is anyhow *not* an intrinsic property of the Josephson junction, because it depends on R , as seen in Eq.(8).

V. MICROWAVE MEDIATED TUNNELING

By irradiating the Josephson junction, depicted in Fig.1, with an electromagnetic microwave of frequency ω , Shapiro observed¹ the step-like characteristic $I(U)$, recalled in Fig.5. The discontinuities of $\frac{d\langle I \rangle}{d\langle U \rangle}$, showing up at $\langle U \rangle = \frac{m\hbar\omega}{2e}$ with $m > 0$ being an integer, brought forward a cogent proof that the MBE state comprises an *even* number of electrons. In order to explain this experimental result, let us begin with studying the microwave induced tunneling of *one* bound electron pair across the $U_m = \frac{m\hbar\omega}{2e}$ biased barrier. The corresponding Hilbert space, describing the system *before* and *after* crossing, is subtended by the basis $\{\varphi_i = \varphi_A(c_e) \otimes \varphi_B(c_e), \varphi_1 = \varphi_A(c_e + \frac{2}{V}) \otimes \varphi_B(c_e - \frac{2}{V})\}$ of respective energies $V\mathcal{E}_i, V\mathcal{E}_i + m\hbar\omega$. The tunneling motion of one electron pair is then described by $\psi_0(t)$,

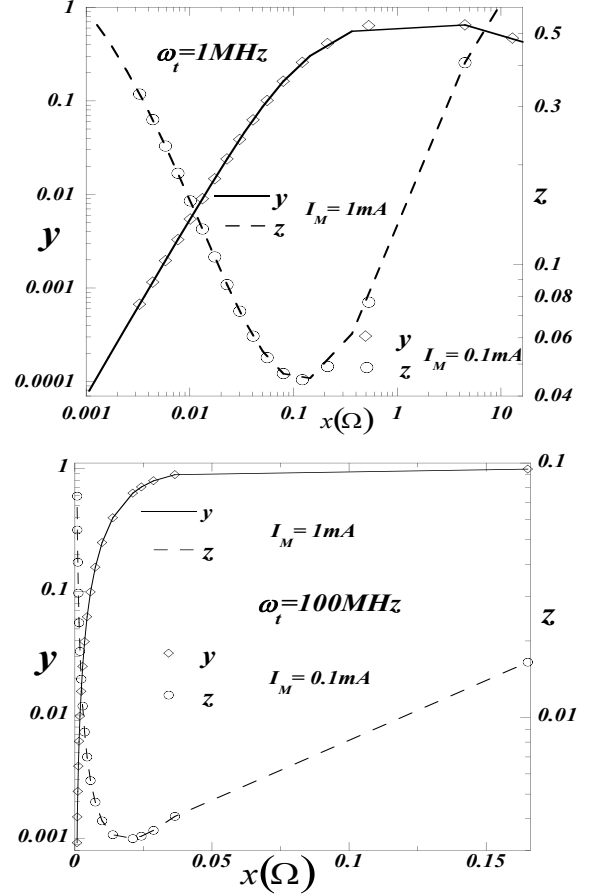


FIG. 4. Logarithmic and semi-logarithmic plots of the characteristics $I(U)$, calculated for $\omega_t = 1\text{MHz}, 100\text{MHz}$, respectively, and $I_M = 1\text{mA}, 0.1\text{mA}$, with $x = \frac{\langle U \rangle}{I_M}$, $y = \frac{\langle I \rangle}{I_M}$, $z = \frac{\langle U \rangle}{U_s}$.

solution of the Schrödinger equation

$$i\frac{\partial\psi_0}{\partial t} = H_0(t)\psi_0 \quad (9)$$

$$H_0 = m\omega\sigma_z + 2(\omega_t + \omega_r \sin(\omega t))\sigma_x$$

The Hamiltonian H_0 is expressed in frequency unit, $\frac{V\mathcal{E}_i}{\hbar} + \frac{m\omega}{2}$ is taken as the origin of energy, ω_r stands for the dipolar, off-diagonal matrix element²⁹ (the microwave power is $\propto \omega_r^2$), and σ_z, σ_x are Pauli's matrices²⁶, projected onto $\{\varphi_i, \varphi_1\}$. It is worth pointing out that Eq.(9) could be readily solved like Eq.(6), if H_0 were t independent. Accordingly, in order to get rid of the t dependence of H_0 , we shall take advantage of a procedure devised for nonlinear optics^{30,31}.

To that end, H_0 is first recast into

$$H_0 = P_0 + f(t)\sigma_x \quad , \quad (10)$$

for which $P_0 = m\omega\sigma_z + 2\omega_t\sigma_x$ is a Hermitian, 2×2 , t independent matrix, such that $(P_0)_{1,1} + (P_0)_{2,2} = 0$, $(P_0)_{2,2} - (P_0)_{1,1} = m\omega$, and $f(t) = \omega_r \sin(\omega t)$ is a real function of period $= \frac{2\pi}{\omega}$, having the dimension of a fre-

quency, such that $\langle f \rangle = \int_0^{\frac{2\pi}{\omega}} f(t) dt = 0$. Then H_0 is projected onto $\{\psi_-, \psi_+\}$, the eigenbasis of P_0

$$G = TH_0T^{-1} = \epsilon\sigma_z + d(t)\sigma_z + g(t)\sigma_x \quad (11)$$

T is the unitary transfer matrix from $\{\varphi_i, \varphi_1\}$ to $\{\psi_-, \psi_+\}$ and σ_z, σ_x have been projected onto $\{\psi_-, \psi_+\}$. The corresponding eigenvalues are $\pm \frac{\epsilon}{2}$ with $\epsilon = \sqrt{(m\omega)^2 + \omega_t^2} \approx m\omega$ because of $\omega_t \ll \omega$, while the real functions $d(t), g(t)$ have the same properties as $f(t)$ in Eq.(10). Let us now introduce^{30,31} the unitary transformation $R_1(t)$, operating in the Hilbert space, subtended by $\{\psi_-, \psi_+\}$

$$R_1(t) = e^{i\Phi(t)} |\psi_-\rangle \langle \psi_-| + e^{-i\Phi(t)} |\psi_+\rangle \langle \psi_+| \quad (12)$$

with the dimensionless $\Phi(t) = \frac{\omega t}{2} - \int_0^t d(u) du$. We then look for $\psi_1 = R_1^{-1}\psi_0$, solution of the Schrödinger equation

$$\begin{aligned} i\frac{\partial \psi_1}{\partial t} &= H_1\psi_1, \quad H_1 = R_1^{-1}GR_1 - iR_1^{-1}\dot{R}_1 \\ H_1 &= P_1 + \Re(z_1(t))\sigma_x + \Im(z_1(t))\sigma_y \\ P_1 &= \epsilon\sigma_z + 2\omega_1\sigma_x \end{aligned} \quad (13)$$

for which the Hermitian 2×2 matrix P_1 has the same properties as P_0 in Eq.(10), except for $(P_1)_{2,2} - (P_1)_{1,1} \approx (m-1)\omega$, $(P_1)_{2,1} = \omega_1 = \omega_r/2$ instead of $(P_0)_{2,2} - (P_0)_{1,1} = m\omega$, $(P_0)_{2,1} = \omega_t$, the Pauli matrices $\sigma_z, \sigma_x, \sigma_y$ have been projected onto $\{\psi_-, \psi_+\}$, and $\Re(z_1(t)), \Im(z_1(t))$ which are the real and imaginary parts of the complex function $z_1(t)$, have the same properties as $f(t)$ in Eq.(10). Consequently, iterating this procedure m of times yields finally

$$\begin{aligned} i\frac{\partial \psi_m}{\partial t} &= H_m\psi_m \\ H_m &= P_m + \Re(z_m(t))\sigma_x + \Im(z_m(t))\sigma_y \\ P_m &= \eta\sigma_z + 2(\Re(\omega_m)\sigma_x + \Im(\omega_m)\sigma_y) \end{aligned} \quad (14)$$

for which the Pauli matrices $\sigma_z, \sigma_x, \sigma_y$ have been projected onto the eigenbasis of P_m , $\{\psi_-, \psi_+\}$, and $\eta \approx 0$, $|\omega_m| \ll \omega_r$. The Fourier series $\Re(z_m(t)), \Im(z_m(t))$ of fundamental frequency ω play no role, because the resonance condition²⁶ $|(P_m)_{1,1} - (P_m)_{2,2}| = \omega$ is not fulfilled due to $|(P_m)_{1,1} - (P_m)_{2,2}| = |\eta| \ll \omega$, so that Eq.(14) is finally solved, similarly to Eq.(6), to give

$$\psi_m = \cos\left(\frac{|\omega_m|t}{2}\right) \psi_- - i \sin\left(\frac{|\omega_m|t}{2}\right) \psi_+ \quad .$$

The solution of Eq.(9) is thereby inferred to read

$$\psi_0(t) = \left(\prod_{i=1,m} R_i(t) \right) \psi_m(t) \quad .$$

U_m can be fitted to get $\eta = 0$. Thus, for the sake of illustration, calculated $|\omega_m|$ and $\delta_m = 1 - \frac{2eU_m}{m\hbar\omega}$ are indicated in table I. As expected, $|\omega_m|$ decreases steeply

TABLE I. calculated $|\omega_m|, \delta_m$ values with $\omega = 10GHz$, $\omega_r = 100MHz$ and $\omega_t = 100MHz, 1MHz$.

	$\omega_t = 100MHz$		$\omega_t = 1MHz$	
m	$\frac{ \omega_m }{\omega_r}$	δ_m	$\frac{ \omega_m }{\omega_r}$	δ_m
1	0.5	2×10^{-4}	0.5	2×10^{-8}
2	5×10^{-5}	8×10^{-5}	5×10^{-7}	3×10^{-5}
3	3×10^{-6}	3×10^{-5}	3×10^{-6}	8×10^{-6}
4	10^{-10}	2×10^{-5}	6×10^{-13}	4×10^{-6}
5	5×10^{-12}	10^{-5}	5×10^{-12}	3×10^{-6}
6	5×10^{-13}	7×10^{-6}	5×10^{-13}	2×10^{-6}
7	5×10^{-13}	5×10^{-6}	5×10^{-13}	10^{-6}
8	7×10^{-13}	4×10^{-6}	7×10^{-13}	9×10^{-7}
9	10^{-12}	3×10^{-6}	10^{-12}	7×10^{-7}
10	3×10^{-12}	3×10^{-6}	3×10^{-12}	6×10^{-7}
11	4×10^{-12}	2×10^{-6}	4×10^{-12}	5×10^{-7}

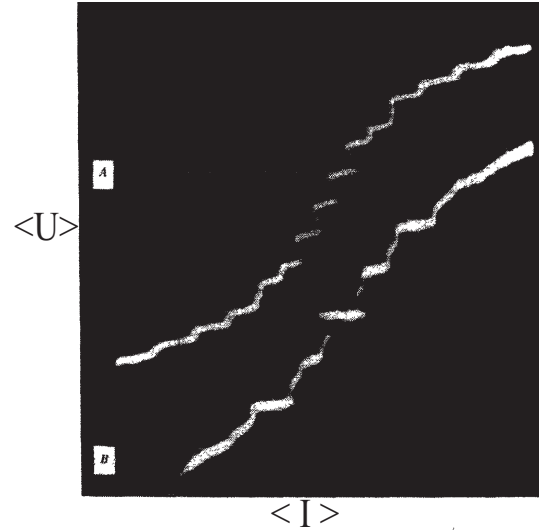


FIG. 5. Characteristics $I(U)$, recorded by Shapiro¹ (used here with APS permission) at 9.3GHz for A (vertical scale is 58.8 pV/cm, horizontal scale is 67 nA/cm) and 24.85GHz for B (vertical scale is 50 pV/cm, horizontal scale is 50 pA/cm).

with increasing m but, remarkably enough, $|\omega_{2m+1}|$ decreases more slowly than $|\omega_{2m}|$, all the more so since ω_t is weaker. This property ensues^{26,29} from $\omega_{2m} = 0, \forall m$ for $\omega_t = 0$.

Let us neglect $\frac{2eU_m}{V\mathcal{E}_i} < 10^{-20}$, so that the energy of ψ_0 is taken to be constant and equal to $V\mathcal{E}_i$. The coherent tunneling of $n \gg 2$ of bound electrons will thence be described by Eq.(7), except for $\{\varphi_i, \varphi_f\}$, $\langle U \rangle - U_m$, $\langle I_m \rangle$, showing up instead of $\{\varphi_i, \varphi_f\}$, $\langle U \rangle$, $\langle I \rangle$, respectively, which entails that $\langle I_m \rangle (\langle U \rangle - U_m) = \langle I \rangle (\langle U \rangle)$, as illustrated by Fig.4. Likewise, the contributions $\langle I_{m=1,2,3,\dots} \rangle$ will add up together to give the step-like characteristic $I(U)$, recalled in Fig.5. At last, Shapiro noticed¹ that

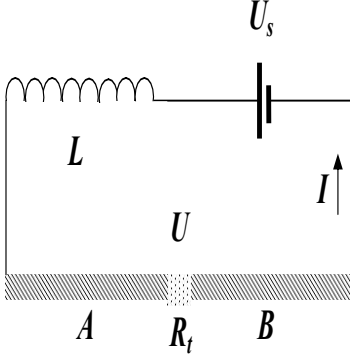


FIG. 6. Sketch of the electrical setup, displaying the negative resistance behaviour. L refers to the self-inductance of the coil.

some contributions $\langle I_m \rangle$ were missing in Fig.5. As explained above in section 4, this might result from the corresponding $|\omega_m| < \omega_p$ and thence would confirm $\omega_t < \omega$.

VI. NEGATIVE RESISTANCE

Signals $U(t), I(t) \propto \sin(\omega t)$, with the RF frequency ω defined by the resonance condition $LC\omega^2 = 1$, have been observed⁹ in the kind of setup, sketched in Fig.6. Due to $\omega \neq \omega_t$, the bound electron tunneling plays no role and the oscillation rather stems from $R_t(I)$ decreasing¹⁶ down to R_n with $|I|$ increasing up to I_M , as indicated in section 4. Accordingly, since the voltage drop across the coil is equal to $L\dot{I}$, the electro-dynamical equation of motion reads

$$I = \frac{U}{R_t} + C\dot{U} \Rightarrow \ddot{U} = \omega^2(U_s - U) - \frac{\dot{U}}{R_t C} \quad (15)$$

Linearising Eq.(15) around the fixed point $U_0 = U_s \Rightarrow I_0 = \frac{U_s}{R_t(I_0)}$ yields the differential equation

$$\ddot{U} = -\omega^2 U - \frac{\dot{U}}{R_e C} \quad (16)$$

with the effective resistance R_e , defined by $R_e = R_t(I_0) + I_0 \frac{dR_t}{dI}(I_0)$. Due to $\frac{dR_t}{dI} < 0$, the fixed point may be unstable in case of negative resistance $R_e < 0$, which will give rise to an oscillating solution of Eq.(15), $U(t) \propto \sin(\omega t)$. As a matter of fact, integrating Eq.(15) leads to the sine-wave, depicted in Fig.7. Note that, unlike $U(t)$ in Fig.3, every harmonic $\propto \sin(m\omega t)$ with $m > 1$ is efficiently smothered by the resonating L, C circuit due to $LC(m\omega)^2 \neq 1$ for $m > 1$. At last, we have checked that Eq.(15) has no sine-wave solution for $\frac{R_0}{R_n} < 50$ or $U_s > R_n I_M$, because those inequalities entail that $R_e > 0$, which corresponds to a stable fixed point of Eq.(16).

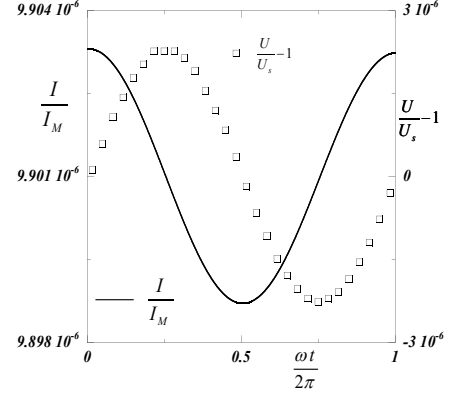


FIG. 7. Plots of the periodic solution $I(t), U(t)$ of Eq.(15), reckoned with $U_s = 10\mu V, I_M = 0.1mA, L = 1\mu H, C = 100pF, \omega = 100MHz$.

VII. CONCLUSION

All experimental results¹, illustrating the Josephson effect, have been accounted for on the basis of bound electrons tunneling periodically across the insulating barrier. Likewise, the very existence of the Josephson effect has been shown to be conditioned by $\frac{\partial \mu}{\partial c_s} < 0$, which had previously been recognized as a prerequisite for persistent currents¹⁵, thermal equilibrium¹⁶, a stable superconducting phase¹⁸ and a second order transition¹⁹, occurring at the critical temperature T_c too. The negative resistance feature⁹ has been ascribed to the tunneling resistance of independent electrons decreasing with increasing current, flowing through the superconducting electrodes, which confirms the validity of an analysis of the superconducting-normal transition¹⁶.

By contrast with this work, $I_n(t), I_s(t)$ are dealt with on the *same footing* in the mainstream view^{8,11-14}, both resulting from the tunneling of independent particles, obeying *Fermi-Dirac* statistics. The only difference appears to be the one-particle density of states, namely either that associated with normal electrons for I_n or Bogoliubov-Valatin^{27,28} excitations for I_s .

The coherent tunneling of bound electrons is thus concluded to be the very signature of the Josephson effect. Furthermore it has two noticeable properties :

- since coherent tunneling has been ascribed in the third section to the properties of a MBE state, the time-periodic tunneling of bound electrons through a thin insulating barrier might be observed on a Josephson capacitor, for which the superconducting electrodes A, B would be replaced by magnetic (ferromagnetic or antiferromagnetic) metals¹⁴;
- the coherent tunneling motion seems to have no counterpart in the microscopic realm. For instance, the electrons, involved in a covalent bond, cannot tunnel between the two bound atoms because of their thermal relaxation toward the bond-

ing groundstate. As for the Josephson effect, the bonding eigenfunction and its associated energy would read $\varphi_b = \frac{\varphi_i + \varphi_f}{\sqrt{2}}$ and $V\mathcal{E}_i - \frac{\hbar\omega_i}{2}$, respectively, but the relaxation from the tunneling state

$\psi(t)$ in Eq.(6) toward φ_b might occur only inside the insulating barrier, which is impossible because the valence band, being fully occupied, can thence accomodate no additional electron.

* corresponding author : jszeftel@lpqm.ens-cachan.fr

- ¹ S. Shapiro, Phys.Rev.Lett., 11, 80 (1963)
- ² S. Shapiro *et al.*, Rev.Mod.Phys., 36, 223 (1964)
- ³ T. Nagatsuma *et al.*, J.Appl.Phys., 54, 3302 (1983)
- ⁴ D. R. Gulevich *et al.*, Prog.In.Electro.Res.Symp., IEEE, 3137 (2017)
- ⁵ B. Douçot and J. Vidal, Phys. Rev. Lett., 88, 227005 (2002)
- ⁶ M. H. Devoret and R. J. Schoelkopf, Science, 339, 1169 (2013)
- ⁷ A. Deville and Y. Deville, Quant.Inform.Process., 18, 320 (2019)
- ⁸ B.D. Josephson, Phys.Lett., 1, 251 (1962)
- ⁹ D.E. McCumber, J.Appl.Phys., 39, 3113 (1968)
- ¹⁰ V.L. Ginzburg and L.D. Landau, Zh.Eksperim.i.Teor.Fiz., 20, 1064 (1950)
- ¹¹ N.R. Werthamer, Phys.Rev., 147, 255 (1966)
- ¹² A. I. Larkin and Y. N. Ovshinnikov, Sov.Phys.JETP, 24, 1035 (1967)
- ¹³ A. Barone and G. Paterno, Physics and Application of the Josephson Effect, ed. John Wiley & Sons (1982)
- ¹⁴ P.L. Lévy, Magnetism and Superconductivity, ed. Springer (2000)
- ¹⁵ J. Szeftel, N. Sandeau and M. Abou Ghantous, Eur.Phys.J.B, 92, 67 (2019)
- ¹⁶ J. Szeftel, N. Sandeau and M. Abou Ghantous, J.Supercond.Nov.Magn., 33, 1307 (2020)
- ¹⁷ J. Szeftel, N. Sandeau, M. Abou Ghantous and A. Khater, EPL, 131, 17003 (2020)
- ¹⁸ J. Szeftel, N. Sandeau, M. Abou Ghantous and M. El-Saba, J.Supercond.Nov.Magn., 34, 37 (2021)
- ¹⁹ J. Szeftel, N. Sandeau, M. Abou Ghantous and M. El-Saba, EPL, 134, 27002 (2021)
- ²⁰ L. Schiff, Quantum Mechanics, ed. McGraw-Hill (1969)
- ²¹ J. Szeftel, N. Sandeau and A. Khater, Phys.Lett.A, 381, 1525 (2017)
- ²² J. Szeftel, N. Sandeau and A. Khater, Prog.In.Electro.Res.M, 69, 69 (2018)
- ²³ J. Szeftel, M. Abou Ghantous and N. Sandeau, Prog.In.Electro.Res.L, 81, 1 (2019)
- ²⁴ J. Bardeen, L.N. Cooper and J.R. Schrieffer, Phys.Rev., 108, 1175 (1957)
- ²⁵ N.W. Ashcroft and N. D. Mermin, Solid State Physics, ed. Saunders College (1976)
- ²⁶ A. Abragam, Nuclear Magnetism, ed. Oxford Press (1961)
- ²⁷ R.D. Parks, Superconductivity, ed. CRC Press (1969)
- ²⁸ J.R. Schrieffer, Theory of Superconductivity, ed. Addison-Wesley (1993)
- ²⁹ R. Boyd, Nonlinear Optics, ed. Academic Press USA (1992)
- ³⁰ J. Szeftel, N. Sandeau and A. Khater, Opt.Comm., 282, 4602 (2009)
- ³¹ J. Szeftel *et al.*, Opt.Comm., 305, 107 (2013)